GEOSTAR SYSTEMS: ADVANCEMENTS IN BOREHOLE HEAT EXCHANGER TECHNOLOGY FOR THE URBAN HEAT TRANSITION - MONITORING AND FUTURE DEVELOPMENTS

Michael Rath[1]*, [2], Timm Eicker[1], Holger Born[1], Jonas Güldenhaupt[1], Gregor Bussmann[1] and Rolf Bracke[1]

[1]Fraunhofer Research Institution for Energy Infrastructures and Geothermal Systems (IEG), Bochum, Germany

[2]Bochum University of Applied Sciences, Department of Civil and Environmental Engineering, Bochum, Germany

*Corresponding Author: michael.rath@ieg.fraunhofer.de

ABSTRACT

Since its first deployment and commissioning in 2013, the GeoStar technology has emerged as a significant solution for addressing the challenges associated with urban heating systems within spatially constrained environments. We are giving a detailed overview of the GeoStar projects located in Bochum, focusing mainly on their energetic behavior and sustained performance, innovative drilling methodologies, and forthcoming operational strategies. GeoStar systems represent an innovative approach to borehole heat exchanger (BHE) technology, designed to optimize thermal energy supply in densely populated urban areas with limited surface area. This methodology involves the drilling of multiple inclined BHEs arranged in a star-shaped configuration from a central drill pad. This approach facilitates efficient extraction and storage of thermal energy beneath existing urban infrastructure, addressing challenges encountered with traditional vertical BHEs. Our presentation includes an analysis of the long-term performance data from the initial GeoStar 1 installation at the Fraunhofer IEG Campus in Bochum. Comprising 17 BHEs supporting four heat pumps for campus heating and cooling, this installation serves as a compelling case study. Furthermore, GeoStar 2, situated at Hochschule Bochum, demonstrates advancements achieved through the integration of advanced borehole drilling techniques, enhancing precision and system efficiency. Both installations are equipped with heat and cooling meters, temperature sensors, and optical fiber technology for distributed in-situ temperature sensing, providing insights into system efficiency and thermal budget management. Looking ahead, our research aims to integrate the operation of heat pump systems with the electricity market. Preliminary work has been initiated, laying the foundation for a more adaptive and market-responsive operation. This forward-thinking approach not only promises to enhance system efficiency but also aligns energy production with market dynamics and renewable energy availability. These advancements offer valuable insights into sustainable urban heating and cooling, providing a model adaptable to similar urban contexts.

1 INTRODUCTION

The debate about phasing out fossil fuels in Germany to meet its climate protection targets by 2045 is ongoing. At the moment, dependence on fossil fuels remains at 67% of the final energy consumption. The heating sector accounts for the largest share of final energy demand in Germany with 56% or around 1,400 TWh/a in 2019 (Bracke et al., 2022). Heat consumption in Germany for space heating (641 TWh/a in 2020) and domestic hot water (131 TWh/a in 2020) has been around 780-800 TWh/a for many years (Born et al., 2022). Following the Federal Climate Protection Act (Federal Climate Protection Act, 2021), CO_2 emissions have to gradually be reduced by 43% from 2020 to 2030, and then to zero by 2045. While a reduction in energy demand for space heating is definitely possible and sensible via refurbishment measures in the existing stock, the complete avoidance of greenhouse gas emissions can only be achieved by moving away from the two fossil fuels natural gas and oil towards an energy system where heat pumps play a crucial role in the heating sector – either in district heating grids (cf. Sporleder et al., 2023a, 2023b and 2024) or in decentralized solutions. And due to the increase of renewable

https://doi.org/10.52202/077185-0206

electricity in the grid, the flexibility will also become more and more important in the thermal sector (cf. Beuker et al., 2021, George et al., 2023, Koch et al., 2024). While district heating solution may be the key in densely populated areas, sometimes they are not economically feasible and still we have spatial constraints. Densely populated areas show the effect of urban heating islands (cf. Chen et al., 2022), which can be seized by the use of geothermal systems (Zhu et al., 2011). The GeoStar geometry (cf. Bussmann et al., 2015) is a highly promising option to optimize the energy provision from borehole heat exchangers (BHE) if space at the surface is limited, as it is typically the case in densely populated urban areas. The concept is based on drilling multiple tilted BHE in a star shaped array from a central drill pad, enabling thermal energy provision from and thermal energy storage into rock volumes located beneath existing infrastructure, not accessible by conventional vertical BHEs. Over the past 10 years, six systems were established - two located in Bochum and four in France. In Bochum, the first implemented two GeoStar systems are used for active heating and passive cooling of the building infrastructure of Fraunhofer IEG (GeoStar 1, cf. Bussmann et al., 2015) and a lecture hall of Bochum University of Applied Sciences (GeoStar 2, cf. Bartels et al., 2018) (cf. Figure 1).

Figure 1: Left: Fraunhofer IEG infrastructure that is supplied by the GeoStar 1. Right: Lecture Hall H9 of Bochum University of applied sciences which is supplied by GeoStar 2

At **GeoStar 1**, 17 BHE were installed on a 6 m x 10 m elliptic area with dipping angles of 10° to 13° up to vertical depths of 190 m (BHE length 200 m). The distance between the borehole starting points on the surface is just 1.5 meters on average. The connection pipes to the central chamber manifold are only 2 m to 4 m long. Hydraulic balancing of the geothermal probes is not necessarily due to different lengths of the connection pipes. Heating and cooling of the IEG campus is performed with four BHE-coupled heat pumps (cf. Figure 3). Furthermore, the cooling demand can be also supplied by passive cooling. The heating load is ~ 140 kW with a heat demand of 252 MWh/a and the cooling load ~ 85 kW with a cooling demand of 51 MWh/a. The performance of the GeoStar is significantly higher than the energy requirements of the connected buildings. This is a result of the research approach and the corresponding research questions. In future, further buildings with a heating capacity of around 50 kW will be connected to Geostar 1.

At **GeoStar 2** (HBO), 12 borehole heat exchangers (BHE) were installed on a circular drill pad with a diameter of 7 m. The inclination of all boreholes is 10°, the depth is 150 m and the average distance between neighboring holes is 8 m. Heating of the HBO lecture hall is performed with a BHE-coupled heat pump. The heating load is ~ 95 kW and cooling load is ~ 55 kW. The cooling demand is supplied by passive cooling. For both GeoStars all BHE are equipped with optical fibers for distributed in-situ temperature sensing. Data collected during the process for both systems include borehole deviations and rock structure (borehole geophysics), thermal conductivity (Enhanced Geothermal Response Tests) and temperature (Fiber Optic DTS).

The French engineering company Celsius Energy has adapted the GeoStar principle for the French market with the help of the Fraunhofer IEG (formerly International Geothermal Centre Bochum) and successfully implemented it in four pilot projects (cf. Celsius Energy, 2024).

In this paper, we are mainly focusing on the energetic behavior, sustained performance and future implementation potential with respect to volatile electricity markets of the GeoStar systems in Bochum.

https://doi.org/10.52202/077185-0206

2 DRILLING PROCESS, DESCRIPTION AND OPTIMIZATION OF THE GEOSTAR IMPLEMENTATION

The pilot site in Bochum is characterized by the following geological situation. Down to a depth of ca. 1000 m the area belongs to Westfal A (Bochum and Witten Formation) and Namur C of the coal bearing Upper Carboniferous. These Upper Carboniferous is characterized by interlayered mudstones, siltstones and sandstones. At irregular intervals interlayered coal seams with variable thicknesses form approximately 5 % of this sequence decreasing with depth. On each slope the geological formations attain a steeply dipping angle of 70° to south-east and to north-west, respectively.

All boreholes were drilled with own equipment and personnel, with the drill unit BO.REX (Bochum Research and Exploration Drilling Rig), a Huette HBR 207 GT (cf. Figure 3 with a total weight of 32 t and a retraction force of 40 t. The drilling itself was done by a hydraulic Down-The-Hole (DTH) hammer system (Wassara) in conjunction with a Kamat high pressure pump (working pressures of maximum 210 bars & nominal flow rate of 600 l/min – see Figure 3.

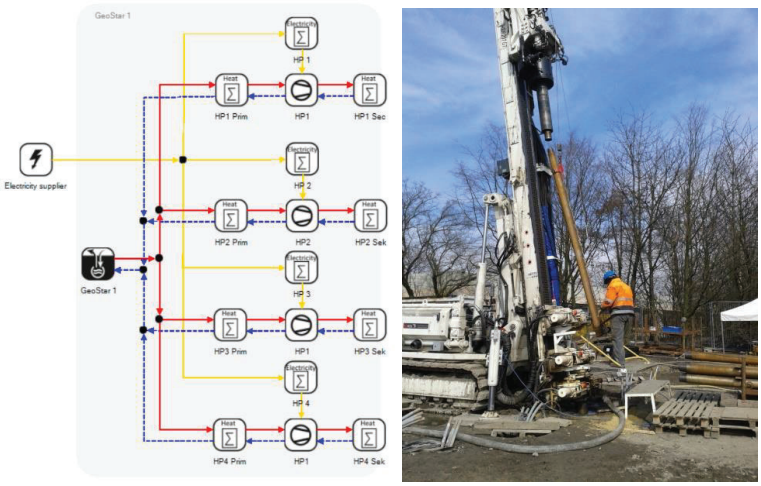

Figure 3: Left: heat pump system with 4 heat pumps attached to GeoStar 1, right: drill rig Bo.Rex - with angled drill carriage

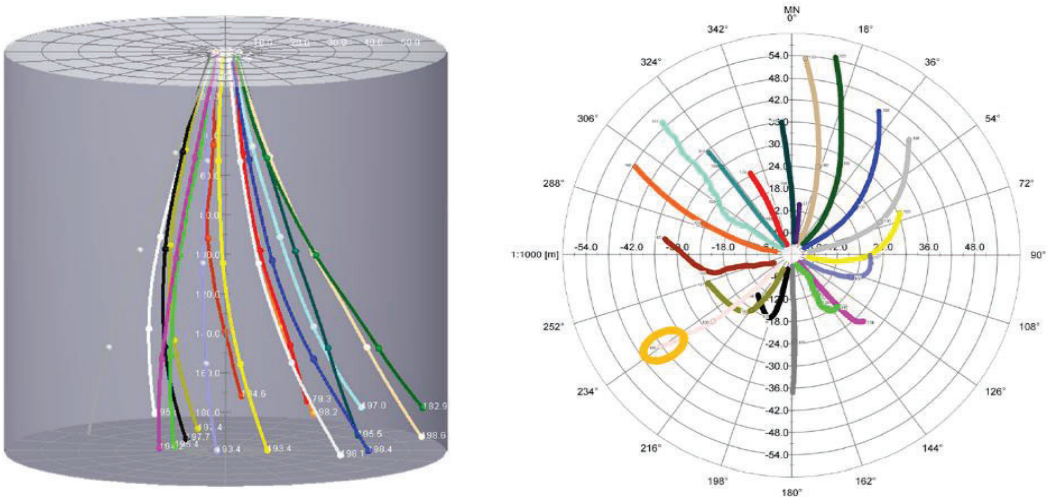

Figure 2: Deviation logs of the GeoStar BHE field; Left: 3-D-presentation, Right: bulls-eye presentation of deviation logs

https://doi.org/10.52202/077185-0206

As a result, 17 BHE (double-U probes, PE-Xa with DIN 40 x 3.7 mm) were successfully drilled and installed with a total length of 3359 m. In addition, three wells have been drilled for additional monitoring purposes. All drill holes were evaluated in a scientific measurement program. Deviation and gamma logs were recorded for all open holes and within each BHE. For future thermal monitoring, all BHEs were equipped with fiber optic cables.

As one can see in Figure 2, a general drift of the boreholes to the NW (perpendicular to the main strike direction of the Upper Carboniferous layer sequence) can be observed. This was caused by the tendency of the drilling tool to align itself perpendicular to the geological formation, as the drilling resistance is lower this way.

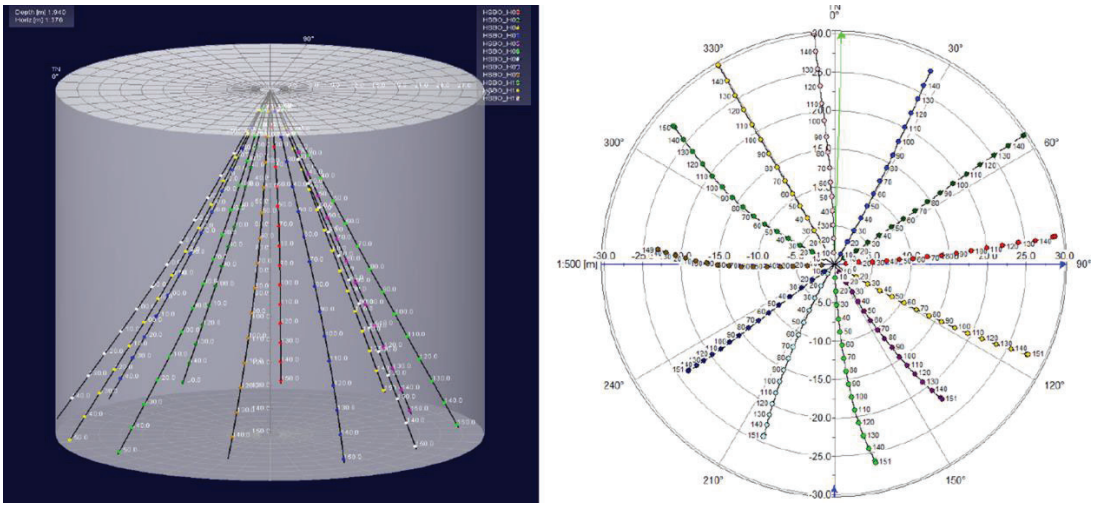

Figure 4: Deviation logs of the GeoStar 2

This did not initially correspond to the desired geometric distribution and arrangement of the BHE. For the thermal system - heat extraction and storage - it was, however, in principle not a hindrance. The tapped volume has not changed significantly compared to the preliminary planning and simulations, as the entire "GeoStar" is slightly tilted downwards. Nevertheless, this behavior of the drill holes, which in principle cannot be controlled during the drilling process, is not desirable. For example, property boundaries could be crossed underground or areas that should be avoided by drilling could be reached. Therefore, some changes were made for the second use case "GeoStar 2.0". The change of drilling method was certainly central, instead of the DTH hammer, a mud drilling method with PCD bits was used.

The drilling equipment was supplemented by

- Heavy rods, which increased the contact pressure in the borehole and thus the directional accuracy of the drilling tool
- Stabilizers, which have improved the guidance of the drill string in the drill hole.

In addition, drilling fluid additives were used to stabilize the borehole and prevent breakouts or collapse. In total, no adjustments that had a significant technical, temporal or economic impact on the drilling progress. However, they did lead to significantly better results. Figure 4 shows that the GeoStar 2.0 has, in principle, achieved the ideal star shape.

In conclusion, it can be stated that the technical feasibility of the GeoStar concept can be safely realized using conventional drilling technology with only minimal adjustments. Where space is limited, particularly in urban structures, this provides a practical option for tapping near-surface geothermal energy for heating and cooling purposes.

https://doi.org/10.52202/077185-0206

3 MONITORING DATA

The GeoStar 2 system is supplying the lecture hall H9 of Bochum university of applied sciences (cf. Figure 1, right image) and is running ever since its installation without failures. The system has recently been extended to be visitable (cf. Figure 5).

Figure 5: GeoStar 2 entrance to the distribution shaft

Monitoring data for GeoStar 1 is available from 2014, in particular we measured the delivered (secondary) heat from each of the four heat pumps, the gained (primary) heat from the GeoStar system for each heat pump, the electricity used by each heat pump and temperatures on the primary and secondary side of each heat pump. In this paper we only take a look into the long-time monitoring data of GeoStar 1, the data of GeoStar 2 will be addressed elsewhere. The data can soon be retrieved from https://www.ieg.fraunhofer.de/de/veroeffentlichungen.html. In Figure 6, we see the amount of heat that is drawn from GeoStar 1, measured with a heat meter at the source side of each heat pump from 2014 until 2022.

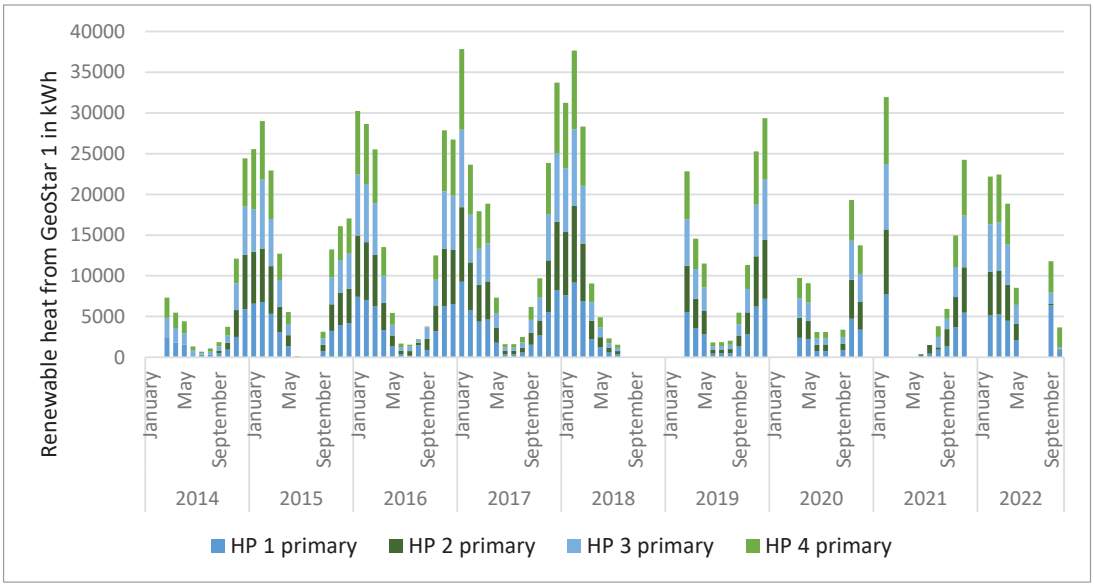

Figure 6: Renewable heat ΔQ_{prim}/kWh from the GeoStar 1 stacked for all heat pumps

https://doi.org/10.52202/077185-0206

While we see some gaps in the data due to communication problems and ring storage overflows, we can nevertheless analyze the meter counting for each heat pumps source side at the beginning of the 104 months measurement period in March 2014 and at the end in October 2022: 1,442,340 kWh of renewable heat have been drawn from GeoStar 1 in that time period. If this amount of heat had been produced by a gas boiler – with natural gas at 240 g CO_2-equivalent/kWh (cf. Federal Ministry for Economic Affairs and Energy, 2019) and 90 % thermal efficiency – it would have been 385 tons of CO_2-equivalent.

In Autumn 2022, the automatic controller unit of the heat pumps failed, leading to manual operation. This opened up the possibility to implement a new controller unit with the possibility to add a high-level control for electricity market-oriented control, which we will address in the next section. It is most of the time straight forward to calculate monthly averaged seasonal performance factors $SPF_{monthly}$ for the heat pumps by dividing the difference of the heat counter at start and end of a month or other period - the so-called counter delta - heat output ΔQ_{sec}, by the used electricity counter delta ΔW i.e.

$$SPF_{monthly} = \Delta Q_{sec}/\Delta W, \quad (1)$$

Figure 7 shows the monthly averaged seasonal performance factor for the time period where it can be calculated. Although sometimes data is missing, the heat pump system seems to have worked reliably all the time.

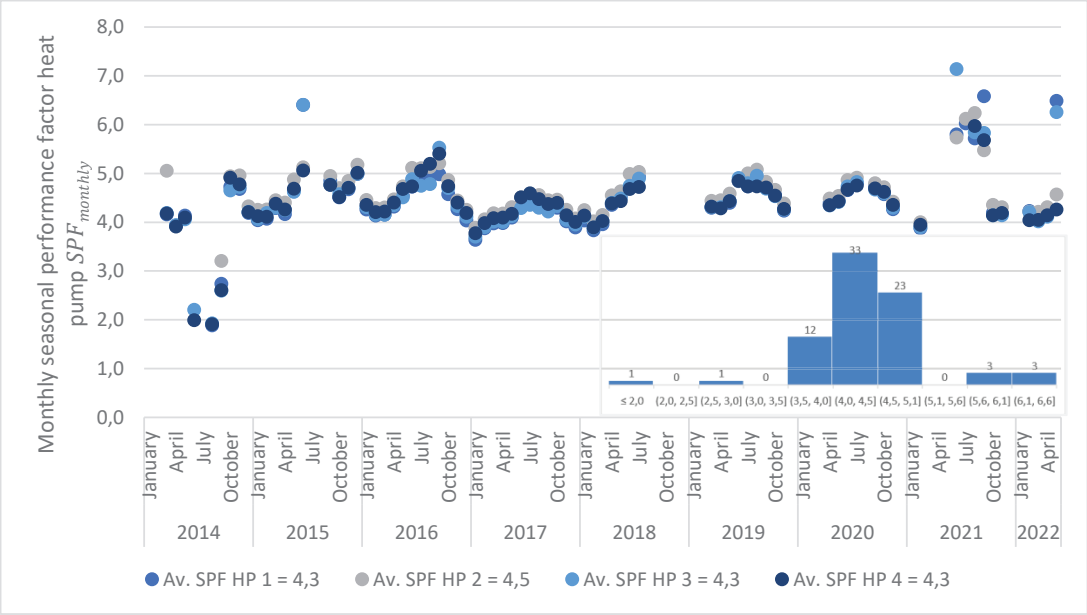

Figure 7: Monthly performance factors for all heat pumps over time and a histogram for the same data for all heat pumps together in the inset showing that $SPF_{monthly}$ of 4,0-4,5 are most likely; the average value for each heat pump is calculated by summing up all available monthly heat deltas and dividing them by the respective sum of all available electricity deltas for each heat pump.

However, if we want to calculate an average the total amount of energy of the whole time period for the used electricity – just like we did above with the renewable ground energy via the counter data at start and end of the period – we have to face that this is not possible in the same way. In Figure 8, we see two completely different graphs for heat pump: the electricity meter was several times exchanged and reset, while the heat meter was not, and we even lack larger time periods, where the electricity meter may or may not have been reset or exchanged. A similar pattern can be found for heat pump 3 – so while we can calculate the performance for heat pump 1 and 3 for several month (cf. Figure 7), we cannot calculate the total amount of electricity in these two cases for the whole operation period exactly, but can only sum up the energy of the months in which we have reliable data.

https://doi.org/10.52202/077185-0206

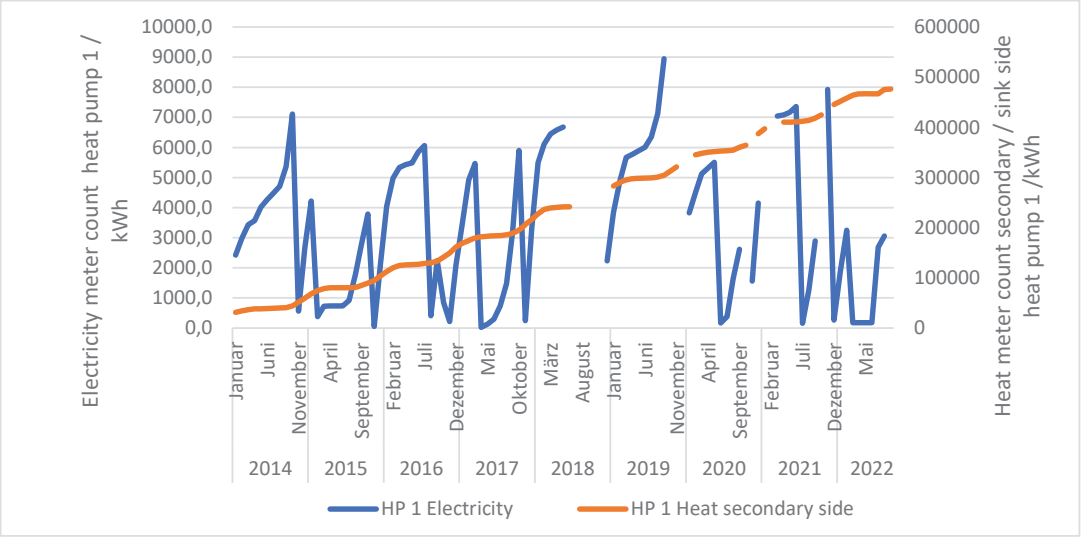

Figure 8: Electricity meter and heat meter count for heat pump 1 – the electricity meter was several times exchanged and reset, while the heat meter was not

However, for heat pump 2 and 4, we have a reliable behavior of the electricity meter and are able to investigate the energy consumed and transferred for the total time period. Since we measure the used electricity ΔW, the output heat ΔQ_{sec} and the renewable heat from the ground ΔQ_{prim} per time period$T$, by neglecting minor heat losses ϵ_{loss}in the heat pump process, we can calculate the seasonal performance factor with in three different ways; equation (1) being the first possibility with index "monthly" replaced by T, i.e. $SPF_{T,s,E} = \Delta Q_{sec}/\Delta W$ with s for secondary and E for electricity, but due to

$$\Delta Q_{sec} + \epsilon_{loss} = \Delta W + \Delta Q_{prim} \tag{2}$$

by substituting ΔW in equation (1), we additionally have

$$SPF_{T,s,p} = \Delta Q_{sec}/(\Delta Q_{sec} - \Delta Q_{prim} + \epsilon_{loss}) \tag{3}$$

and by substituting ΔQ_{sec} in equation (1), we obtain

$$SPF_{T,p,E} = (\Delta W + \Delta Q_{prim} - \epsilon_{loss})/\Delta \mathrm{W}. \tag{4}$$

When omitting ϵ_{loss}>0, for heat pumps it can be shown that

$$SPF_{T,s,E} < SPF_{T,p,E} < SPF_{T,s,p} \tag{5}$$

When incorporating the loss effect, all equations – (1), (3) and (4) are equivalent and of the form $SPF_T = n/p$. To assess the effect on the equations when setting $\epsilon_{loss} \approx 0$, we add ϵ_{loss} to the nominator n of equation 4 and subtract it in the denominator d of equation 3. Equality for $n, d, \epsilon_{loss} > 0$ would only be possible if $\frac{n+\epsilon_{loss}}{d} = \frac{n}{d-\epsilon_{loss}} \Leftrightarrow d - n = \epsilon_{loss}$. But since we are talking about heat pumps, we have $n > p$ always and thus never equality for $\epsilon_{loss} > 0$, instead we have $\frac{n}{d} < \frac{n+\epsilon_{loss}}{d} < \frac{n}{d-\epsilon_{loss}}$ and thus $SPF_{T,s,E} < SPF_{T,p,E} < SPF_{T,s,p}$, □.This makes $\mathrm{SPF}_{\mathrm{T,s,p}}$ and $SPF_{T,p,E}$ upper bounds for $SPF_{T,s,E}$, the actual performance factor. In Table 1, the results are listed – especially the results of heat pump 2 cluster closely together and confirm the results from Figure 7.

https://doi.org/10.52202/077185-0206

Table 1: Measured energies and Seasonal performance factors

Data relates to time period T 03/2014-10/2022	Heat primary (source) side / kWh	Electricity usage / kWh	Heat secondary (sink) side / kWh	$SPF_{T,s,E}$	$SPF_{T,s,p}$	$SPF_{T,p,E}$
Heat pump 1	356,160	-	445,010	-	5,01	-
Heat pump 2	349,220	103,063	448,740	**4,35**	**4,51**	**4,39**
Heat pump 3	361,000	-	447,980	-	5,15	-
Heat pump 4	375,960	110,463	461,110	4,17	5,42	4,40

In Figure 9, we see a daily sampled temperature curve for the flow and return flow temperatures from and to the GeoStar 1, and histograms for the same two temperatures from approximately 10^6 data records in Figure 10 – also after nearly a decade of operation, the temperatures have a quite good average level.

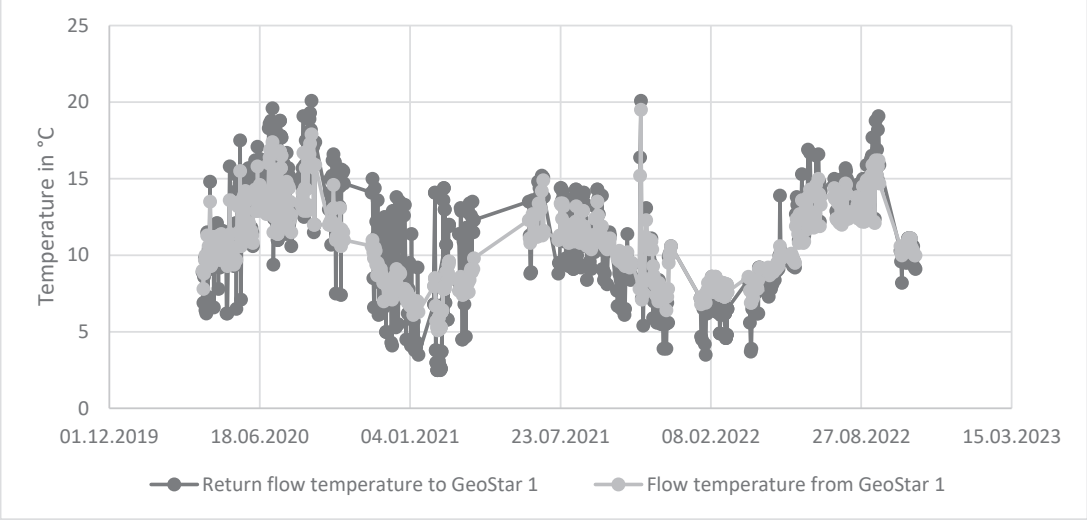

Figure 9: Daily sampled temperatures for flow and return flow of GeoStar 1

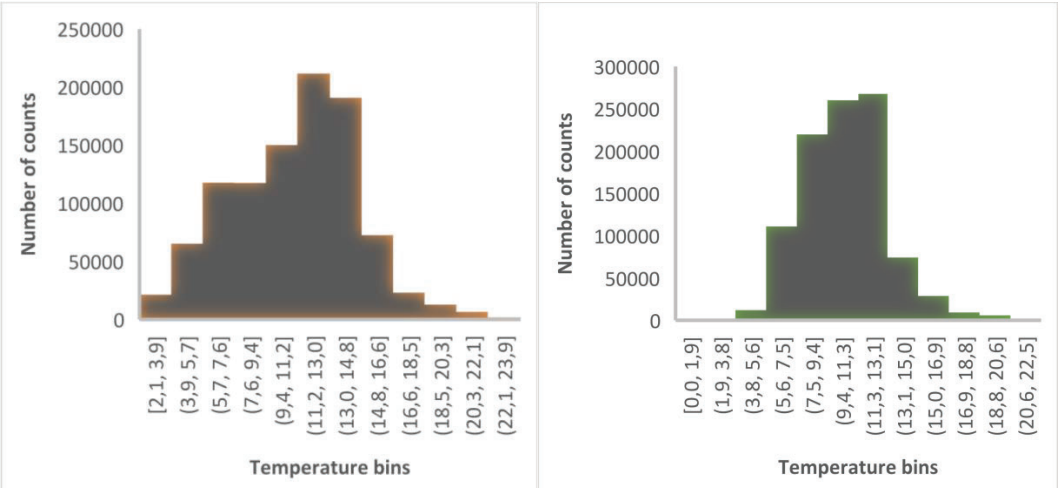

Figure 10: Histograms of approximately 10^6 data records in minute resolution from the period 4/2019 - 11/2022; Left: return flow temperature of GeoStar 1, Right: flow temperature of GeoStar 1

https://doi.org/10.52202/077185-0206

In ***Table 2***, there are average condenser and evaporator temperatures, i.e. the averages of flow and return flow temperatures on each side of the heat pump, evaluated only when the respective heat pump is running, and Carnot efficiency η. The data relates to the time period 04/2020-6/2022. The results with the Carnot efficiency also match the seasonal performance factors; e.g. for heat pump 2, we have a Carnot efficiency of 10,35 and a SPF of 4,35, translating to a heat pump grade of 0,42. That is not great, but plausible and acceptable with respect to the age of the system.

Table 2: Average condenser and evaporator temperatures and Carnot efficiency η.

related time period: 04/2020-6/2022	**HP 1**	**HP 2**	**HP 3**	**HP 4**
Average condenser temperature / °C	36,37	36,54	36,27	36,36
Average evaporator temperature / °C	7,82	6,62	6,83	6,66
Carnot efficiency *η*	10,84	10,35	10,51	10,42

4 ELECTRICITY MARKET ORIENTED CONTROL

As described in Rath, 2023, we plan to establish an EMPC, i.e. an electricity market-oriented control system for the Fraunhofer IEG Energy Campus (cf. Figure 11) where the GeoStar 1 system is located, and another GeoStar is in the planning stage. Next, we introduce the building bricks of an electricity market-oriented control.

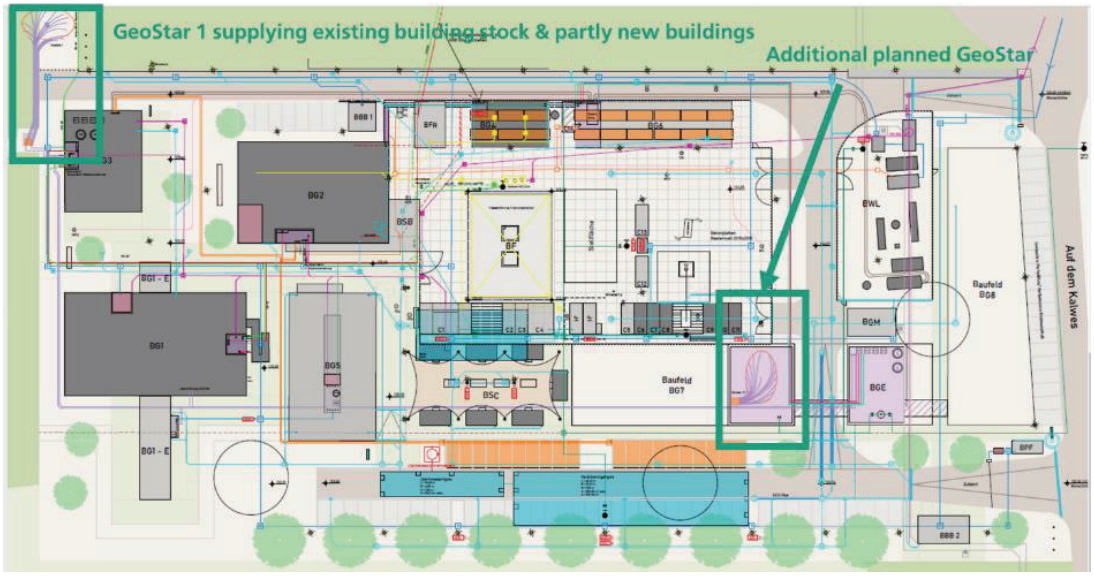

Figure 11:Site plan of exiting (dark grey) and planned buildings (light grey); additional to GeoStar 1, another Geostar is planned to supply the new buildings

In Figure 12, the building bricks and the process flow of the MPC is illustrated (cf. also Rath et al, 2022). It includes

1. The GeoStar site in operation with an existing classical PLC (Programmable Logic Controller), classically ensuring security of thermal supply.
2. An (optionally existing) SCADA (supervisory control and data acquisition) system, which can serve as an interface to the MPC (cf. no.8 in Figure 12)
3. A monitoring database (DB) embedded in a cloud infrastructure with a system for cleaning, collecting and storing data, serving also to supervise the effectiveness of the MPC
4. The intelligent core of the MPC - the Model: Utilizing the collected data from the data base, this can be used to predict demand and supply and to evaluate uncertainties. A whole range of models

https://doi.org/10.52202/077185-0206

can be employed, ranging from detailed physical white box models to black box models built by training regression type machine learning models with data, and grey box models which lie in between.

5. Stochastic operation plan optimization with weather-based forecasts that can predict the demand for the following day, and optimize its operation plan with respect to operational expenditure or CO_2-emissions (cf. Rath *et al*, 2022).
6. Connected external services, i.e. spot market price signals, weather forecasts, and potentially variable grid fees
7. The output of the operation plan and secure transfer to the high-level control while keeping the system safe and resilient.
8. The high-level control receiving the optimized operation plan either directly from the cloud infrastructure or the SCADA system, delivering it via the MPC interface to the classical PLC.

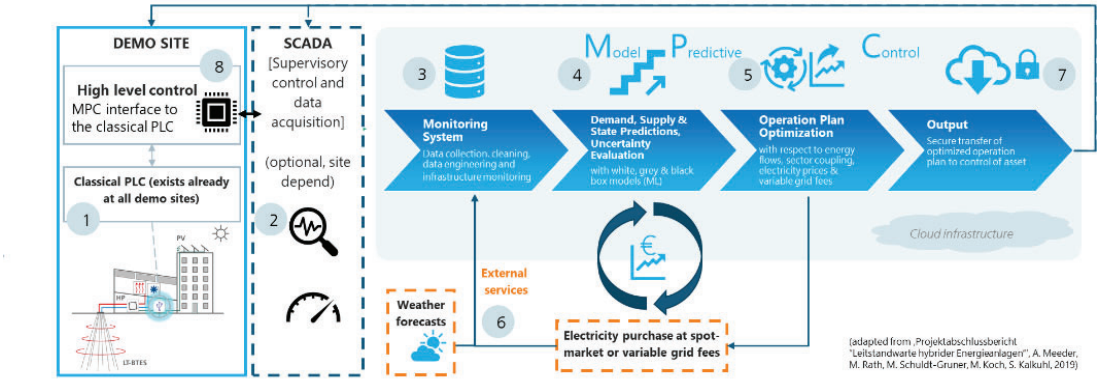

Figure 12: MPC – Process flow which will be implemented or completed at every of our existing demo sites.

The CAPEX for implementing an MPC may of course vary depending on the complexity of the plant. But to roughly estimate the operational saving potential, we take the following assumptions: In the future, there will be heat pumps on the campus with a total thermal output of approx. 0.4 $MW_{thermal}$. We assume an SPF of 4 and thus an electric power consumption of approximately 0.1 MW. We should be able to buffer 2 hours of full load; thus, we take the buffer storage volume to be 0.8 MWh (approx. 36 m³). And finally, minimum running and downtimes for the heat pumps are set to 45 min each. With these assumptions, we run 20,000 simulations of random operation plans at the test date 16th of October, 2023 (cf. Rath, 2023) and as the largest integral 199.75 €, (cf. Figure 13, right hand-side, and left hand-side,) the smallest integral 174.5 €. The mean of all simulations gives 188.68 €, and the median of all simulations results in 188.91 €. So, taking the smallest schedule with respect to the mean, we save 14.18 €, which is 7.5 %. With Savings of 14.18 € per day, we approximately save per year (365d) approx. 5,2 T€/a.

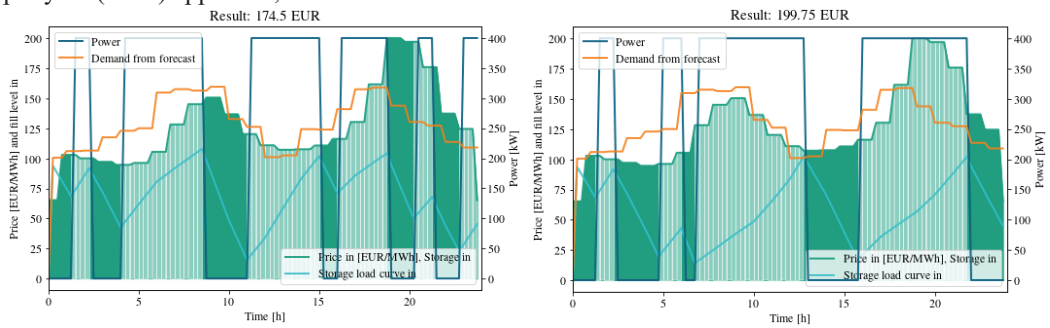

Figure 13: Left: cheapest operation plan, right: most expensive operation plan

The shift towards a decentralized energy transition is unmistakably underway, characterized by the emergence of decentralized, multivalent systems boasting a significant proportion of renewable

https://doi.org/10.52202/077185-0206

energy sources. This trend is set to define the energy landscape of the future. However, to achieve a seamless transition to 100% renewable energy, it's imperative that our energy systems exhibit flexibility. This flexibility enables them to adeptly respond to fluctuations and demands inherent in renewable energy sources. Leveraging machine learning for increasingly accurate predictions becomes crucial in this regard. By harnessing predictive analytics, we can optimize scheduling for energy facilities, ensuring efficient operation. Moreover, the integration of predictive maintenance strategies, coupled with anomaly detection techniques, can preemptively address potential system failures. This proactive approach not only enhances operational efficiency but also bolsters the resilience of the energy system as a whole, mitigating risks and ensuring reliable energy supply.

5 CONCLUSION AND OUTLOOK

In this paper, we explained the innovative GeoStar system exemplified by its first two systems located and in operation in Bochum for quite a while. Presenting some encouraging long-term operational data, we think this solution has great potential for the existing building stock – all heat pumps show similar energetic behavior and perform mainly in a range between 4,0 and 4,5. Especially in the context of sector coupling, to drive such systems flexible is one of the key answers to the ever-increasing amount of volatile renewable energies in our energy system. In conclusion, the GeoStar and its subsequent developments represent innovative solutions for urban heat transitions. The long-term monitoring data from both installations form a robust foundation for evaluating the sustainability and efficiency of these systems. Given the availability of many measurements over years, changes in soil temperature due to the system operation could be evaluated and possibly compared with the effects of traditional systems with vertical layout in the future. The forthcoming integration with the electricity market signifies a forward-thinking approach to urban energy management.

REFERENCES

Bartels, N., Bussmann, G., Ignacy, R., 2018, Geothermal Energy in the Context of the Energy Transition Process, International IEEE Conference and Workshop in Óbuda on Electrical and Power Engineering (CANDO-EPE), Budapest, Hungary, 2018, pp. 000103-000108, doi: 10.1109/CANDO-EPE.2018.8601144

Beuker S., Doderer, H., Funke, A., Koch, C., Kondziella, H., Hartung, J., Maeding, S., Medert, H., Meyer-Braune, G., Rath, M., Rogler, N., 2021, Summary report – Flexibility, markets and regulation. https://www.windnode.de/fileadmin/Daten/Downloads/FMR_eng.pdf

Born, H., Bracke, R., Eicker, T., Rath, M., 2022, Roadmap for Near-Surface Geothermal Energy. Fraunhofer IEG. https://doi.org/10.24406/publica-552

Bracke, Rolf, and Ernst Huenges, eds. 2022, Roadmap for Deep Geothermal Energy for Germany, https://doi.org/10.24406/publica-248

Bussmann, G., Bracke, R., Eicker, T., Wittig, V., Tuente, H., Gueldenhaupt, J., Groening, L., Kiel, F.E., Maeggi, K., & Montag, B., 2015, Geostar - a Scalable Borehole Heat Exchanger Plant for Growing District Heating Systems and Constricted Large Urban Infrastructures. *In:* World Geothermal Congress, 16-24 April 2015, Australia-New Zealand, Melbourne, 2015, Published. [Online]. Available: https://pdfs.semanticscholar.org/eceb/d4d75ed0e49f217631327b821c8761b24b83.pdf?_ga=2.84919450.202009135.1592397950-1606601794.1592397950

Celsius Energy, 2024, *Projects - Celsius Energy*, https://www.celsiusenergy.com/en/projects/ [2024-03-14]

Chen, Y., Shan, B., Yu, X., 2022, Study on the spatial heterogeneity of urban heat islands and influencing factors, Building and Environment, Volume 208, 2022, 108604, ISSN 0360-1323, https://doi.org/10.1016/j.buildenv.2021.108604

Federal Climate Protection Act, 2021 (KSG 2021, Erstes Gesetz zur Änderung des Klimaschutzgesetzes vom 18.08.2021, BGBl. I S. 3905

Federal Ministry for Economic Affairs and Energy, 2019, Building Energy Act (Gesetz zur Vereinheitlichung des Energieeinsparrechts für Gebäude und zur Änderung weiterer Gesetze, Gebäudeenergiegesetz, GEG) Bundesgesetzblatt Jahrgang 2020 Teil I Nr. 37, 13.08.2020, p. 1728

https://doi.org/10.52202/077185-0206

George, K. N., Rath, M., Bracke, R., 2023, Quantifying demand flexibilities of buildings for an optimal design and operation of integrated district energy systems. *In:* Proceedings of ECOS 2023 - 36TH International Conference on Efficiency, Cost, Optimization, Simulation and Environmental Impact of Energy Systems, June 25-30, 2023, Las Palmas de Gran Canaria, Spain, https://doi.org/10.52202/069564-0310

Koch, J., Bensmann, A., Eckert, C., Rath, M., Hanke-Rauschenbach, R., 2024, Planning of Reserve Storage to Compensate for Forecast Errors, Energies 17, no. 3: 720. https://doi.org/10.3390/en17030720

Meeder, A., Rath, M., Schuldt-Gruner, M., Koch, M., Kalkuhl, S., 2019, Leitstandwarte hybrider Energieanlagen, Project Completion report, funding code BENE 1137-B5-O https://www.berlin.de/sen/uvk/_assets/umwelt/foerderprogramme/berliner-programm-fuer-___nachhaltige-entwicklung-bene/bene-projekte/bene-1137_abschlussbericht_pbl.pdf

Rath, M., Ray, H., van Treek, M., Meeder, A., 2022, Untersuchung verschiedener Lastprognoseverfahren für die prognosebasierten Steuerung dezentraler Energieanlagen, *Proceedings of BauSim Conference 2022: 9th Conference of IBPSA-Germany and Austria*, ISBN: 978-3-00-073975-0, https://doi.org/10.26868/29761662.2022.70

Rath, M., 2023, Strommarktorientierte Betriebsplanung- und Optimierungsstrategie der geothermischen Wärmepumpensysteme des Energiecampus am Bochumer Standort des Fraunhofer IEG, Der Geothermie Kongress 2023

Sporleder, M., Rath, M., Jansen, M., & Mann, R., 2023a, Chapter 15: A mixed-integer linear programming approach for an optimal-economic design of renewable district heating systems: a case study for a German grid, *In:* Handbook on the Economics of Renewable Energy. Cheltenham, UK: Edward Elgar Publishing. Retrieved Aug 26, 2023, from https://doi.org/10.4337/9781800379022.00024

Sporleder, M., Rath, M., Ragwitz, M., 2024, Solar thermal vs. PV with a heat pump: A comparison of different charging technologies for seasonal storage systems in district heating networks, Energy Conversion and Management: X, 100564, ISSN 2590-1745, https://doi.org/10.1016/j.ecmx.2024.100564

Sporleder, M., Rath, M., Xu, Y., van Beek, M., Ragwitz, M., 2023b, Utilizing Historical Operating Data to increase Accuracy for Optimal Seasonal Storage Integration and Planning. In Proceedings of ECOS 2023 - 36TH International Conference on Efficiency, Cost, Optimization, Simulation and Environmental Impact of Energy Systems, June 25-30, 2023, Las Palmas de Gran Canaria, Spain, https://doi.org/10.52202/069564-0202

Zhu, K., Blum, P., Ferguson, G., Balke, K.-D., Bayer, P., 2011, The geothermal potential of urban heat islands, Environmental Research Letters, vol. 6, no. 1, pp. 019501, doi: 10.1088/1748-9326/6/1/019501

ACKNOWLEDGEMENT

We want to thank all individuals and organizations who helped during the course of planning, engineering, building and monitoring the GeoStar 2.0: Stephan Exner for project oversight, Axel Günter for safety engineering, Lars Heimann for electrical engineering, Detlef Herkt for mechanical workshop (power supply), Wilhelm Hoffmann from the technical service, Jennifer Jacob and Phillip Nachtigal for construction management of the lecture hall construction, Sebastian Michels for drill point calibration, Max Nonnenmacher and colleagues from the carpentry workshop, the Post Office for enduring noise disruptions, Jan Stracke from the electrical workshop, Jascha Börner for assistance with drilling work, Vitalii Samus for the preliminary design of lid, tables, and benches, Niklas Geißler for the first drafting of distribution shaft, Kai Hoffmann for detailed planning for wood and steel construction, Stefan Hohage for sensor wiring, Torsten Wiesend for electrical work, Roman Ignacy, Alexander Krupp, Jonas Lehmann, Henry Tünte and Michael Hannig for monitoring, Matthias Lis for assistance with drilling work and fiber optics, Osman Macit for drilling work, representatives from Henze, Wickelrohr for their donation, representatives from Kubatec, Schachtbau for their donation, Till Paul for container services, Ferdinand Stöckert for geophysical survey, Marcus Thönnessen for steel construction, and also we thank all unnamed contributors who supported this endeavor.

 https://doi.org/10.52202/077185-0206